Self-Diffusion and Viscosity of Low Molecular Weight Polystyrene over a Wide Temperature Range

Osamu Urakawa

Department of Macromolecular Science, Graduate School of Science, Osaka University, Toyonaka, Osaka 560-0043, Japan

Stephen F. Swallen and M. D. Ediger*

Department of Chemistry, University of Wisconsin—Madison, Madison, Wisconsin 53706

Ernst D. von Meerwall

College of Polymer Science and Polymer Engineering, University of Akron, Akron, Ohio 44325

Received August 14, 2003; Revised Manuscript Received November 26, 2003

ABSTRACT: The self-diffusion coefficient D and the viscosity η of low molecular weight polystyrene (1.9×10^3 g/mol) have been measured from $T_g + 3$ °C to $T_g + 160$ °C. Forward recoil spectrometry (FReS) and pulsed-gradient spin-echo NMR methods were combined to determine D values covering more than 10 orders of magnitude. Over this range, D has the same temperature dependence as T/η, to within 1 decade. The small difference can be explained by the different temperature dependences of segmental and terminal relaxation near T_g. The product of D and the terminal relaxation time is independent of temperature over the entire temperature range to an excellent approximation. In contrast, the analogous quantity for low molecular weight glass-forming liquids can increase by several orders of magnitude as T_g is approached from above. This difference is interpreted in terms of the length scale of the spatially heterogeneous dynamics which develop near T_g.

Introduction

Spatial heterogeneity in dynamics near the glass transition temperature T_g has been invoked to explain several striking experimental observations in polymer melts and supercooled liquids.[1,2] For example, the nonexponential decay of relaxation functions for local processes can be a consequence of this heterogeneity since heterogeneous environments give rise to a distribution of relaxation times.[3] The heterogeneous scenario can also explain the enhancement of the translational diffusion coefficient D observed for low molecular weight probe molecules dispersed in glass-forming liquids.[4] Probe diffusion is found to have a weaker temperature dependence than the viscosity η or the probe rotational correlation time τ_c. Small molecules are expected to translate through mobile regions rapidly while rotational motion and the viscosity are more significantly influenced by the slowest regions.[5] The enhancement of translational motion can be quantified by two products which compare the temperature dependence of diffusion to either the rotational correlation time or the viscosity: $D\tau_c$ and $D\eta/T$. While these two variable combinations are expected to be temperature independent for a homogeneous system, for probes in polymers or in low molecular weight glass formers, $D\tau_c$ and $D\eta/T$ can increase by several orders of magnitude as T_g is approached from above.[1,6,7] Very recent work has shown that this enhancement of translational motion is also apparent in *self-diffusion* near T_g for a single-component glass-former, 1,3-bis(1-naphthyl)-5-(2-naphthyl)benzene (TNB).[8] For this system both $D\tau_c$ and $D\eta/T$ are 400 times larger at T_g than at high temperatures.

Should the self-diffusion of a polymer chain also be enhanced due to spatially heterogeneous dynamics? Recent optical experiments by Veniaminov et al.[9] raise this possibility. They report substantial center-of-mass translational mobility for high molecular weight ($>10^5$ g/mol) poly(methyl methacrylate) more than 20 °C below T_g and suggest that spatially heterogeneous dynamics may be responsible. Recent computer simulations by Varnik and Binder[10] on a polymer with 10 beads also suggest the possibility of enhanced polymer diffusion due to heterogeneous dynamics; they found a small enhancement of diffusion (less than a factor of 2) relative to viscosity already at temperatures far above T_g. On the other hand, data from probe diffusion in polymer matrices leads to the expectation that no enhancement of translational mobility should occur in the self-diffusion of high molecular weight polymers. Experiments on probes have shown that both $D\tau_c$ and $D\eta/T$ become increasingly temperature independent as the size of the probe molecule increases.[6,11] This has been interpreted as resulting from spatial and temporal averaging; if different parts of the probe are simultaneously experiencing different dynamic environments, the probe will not be able to move large distances through mobile regions. This type of averaging would also preclude enhanced translational diffusion of polymer chains, especially for high molecular weight polymers.

To our knowledge, there are no data in the literature that allow a definitive test for enhanced translational diffusion in polymer chains. Most polymer diffusion studies were designed to examine the validity of theoretical models related to the global chain motion (e.g., tube models and their alternatives), and especially the molecular weight dependence of diffusion has been studied.[12] In contrast, little is known about the temperature dependence of D near T_g,[13] probably due to the experimental difficulty of such measurements. For

* Corresponding author.

10.1021/ma0352025 CCC: $27.50
Published on Web 01/17/2004

instance, in the case of forced Rayleigh scattering, the polymers are labeled with photoreactive molecules; high molecular weight polymers are used to eliminate the influence of the label. Measurements near T_g are then difficult because of very slow diffusion. On the other hand, depth profiling methods such as forward recoil spectrometry (FReS),[14] secondary ion mass spectroscopy,[15] and neutron reflectivity[16,17] have been used to observe changes in the concentration profiles for polymer bilayer films (typically deuterio/protio bilayers have been used) following annealing-induced diffusion. These methods determine diffusion without photolabeling, and in principle, such techniques can be used to measure diffusion in low molecular weight samples. However, because of low mechanical strength, it is difficult to construct bilayer films of low molecular weight polymers by floating spin-coated thin films off an air/water interface.

Here we report diffusion measurements for low molecular weight polystyrene (PS, $M_w = 1.9 \times 10^3$ g/mol) over a wide temperature range, down to $T_g + 3$ °C. FReS measurements are used at low temperature; a trilayer film including a high molecular weight PS layer as a support allowed the construction of the samples. These low-temperature diffusion measurements are combined with high-temperature data from pulsed-gradient spin-echo NMR to obtain diffusion coefficients spanning 10 decades. Although these PS chains are small (average end-to-end distance is about 3 nm[18]), they are roughly the same size as the regions of slow dynamics reported for a number of liquids by solid-state NMR[19−22] (1−4 nm). Thus, any enhancement effect associated with heterogeneous dynamics might be expected to be substantially attenuated due to spatial averaging.

For these low molecular weight PS chains, we find that D has nearly the same temperature dependence as T/η. The small difference can be explained by the different temperature dependences of segmental and terminal relaxation near T_g. The product of D and the terminal relaxation time is independent of temperature over the entire temperature range to an excellent approximation. These results imply that even chains with only 17 repeat units are sufficiently long that any effects of spatially heterogeneous dynamics are averaged out and do not influence comparisons of different quantities sensitive to global chain dynamics.

Experimental Section

Sample Characterization. Low molecular weight protiopolystyrene and deuteriopolystyrene were purchased from Scientific Polymer Products, Inc., and Polymer Source, Inc., respectively. As supplied, their weight-average molecular weights (M_w) (manufacturer's values) were 1740 and 2300 g/mol, respectively, and the T_g difference for these two samples measured by DSC was 7 °C; T_g is a strong function of molecular weight for low molecular weight PS.[23] High molecular weight deuteriopolystyrene (d-PS-high; M_w = 704 000 g/mol) was purchased from Polymer Source, Inc., and used as received.

For this study it is necessary to match the dynamics of the two low molecular weight polystyrenes; we used T_g as our criterion and adjusted molecular weight to achieve identical T_g's. We fractionated the protiopolystyrene sample several times to increase its average molecular weight by using methyl ethyl ketone (MEK) (solvent)/methanol (nonsolvent). The deuteriopolystyrene was used after one precipitation from MEK/methanol. The fractionated samples were used in all diffusion experiments and are designated as h-PS and d-PS.

The molecular weight distributions of h-PS and d-PS were determined by two methods: matrix-assisted laser desorption/ionization mass spectroscopy (MALDI−TOF) and size exclusion chromatography (SEC) equipped with a viscometry detector for universal calibration. For the MALDI measurement, indoleacrylic acid was used as a matrix with a small amount of silver trifluoroacetate. Figure 1 shows the MALDI−TOF results of h-PS (a) and d-PS (b); these results represent the fractionated samples used in the FReS experiments. The highest peaks of h-PS and d-PS correspond to 17-mers and 16-mers, respectively, and the number-averaged degrees of polymerizations (DP) are calculated to be 17.5 and 17.0, respectively. The number-average DPs determined by SEC (chain ends were assumed to be butyl and hydrogen for both samples) are only slightly different, 16.2 and 16.8 for h-PS and d-PS, respectively. The molecular weight characteristics of the samples used in the FReS experiments are summarized in Table 1. A detailed analysis of the MALDI spectrum is consistent with completely protio end groups for d-PS and an overall deuteration level of 91%, including the influence of end groups.

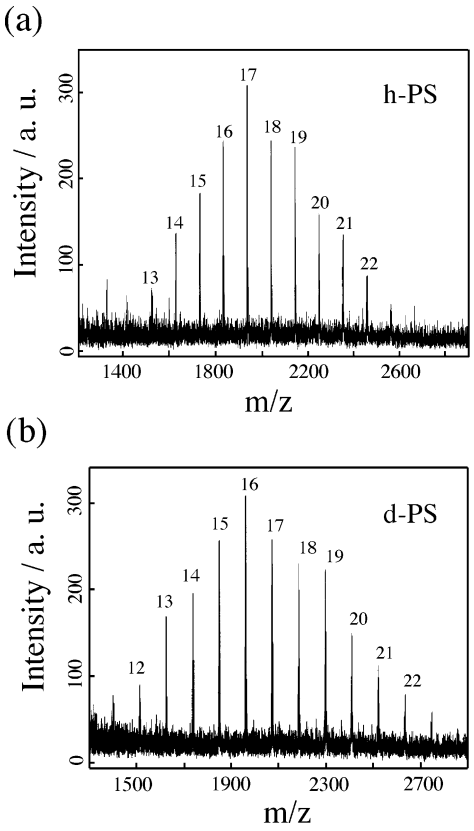

Figure 1. MALDI−TOF spectrum for h-PS (a) and d-PS (b), showing the very similar molecular weight distributions for the two polymers used in the diffusion experiments. Each peak corresponds to the mass of a polystyrene chain plus the mass of one silver ion.

Table 1. Sample Characterization

	$10^{-3}M_w$/g mol^{-1}		M_w/M_n		
code	MALDI	SEC	MALDI	SEC	T_g /°C
h-PS	1.93	1.80	1.03	1.03	59.0
d-PS	2.02	2.02[a]	1.03	1.04	59.5
d-PS-high	704[b]		1.05[b]		

[a] Determined from universal calibration curve using viscometry. [b] Manufacturer's values.

DSC. DSC measurements were carried out with a Seiko Instruments SSC/5200. Cooling scans of d-PS and h-PS are shown in Figure 2. The glass transition temperature T_g was determined as the midpoint of the transition during cooling with a scanning rate of 10 K/min; these values are listed in Table 1. As indicated in Table 1 and Figures 1 and 2, the

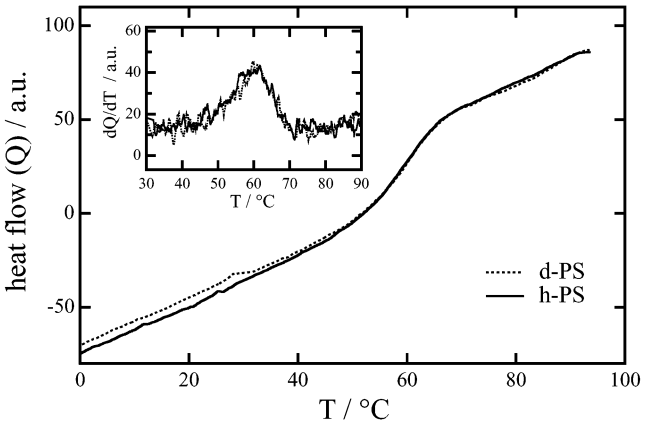

Figure 2. DSC traces for the d-PS and h-PS samples obtained during cooling. The inset shows the differential functions d*Q*/d*T*. The two samples have very similar dynamics as indicated by the very similar DSC traces.

deuterio and protio samples are well matched in terms of molecular weights and T_g values.

Trilayer Sample Preparation. As shown in Figure 3, trilayer films for FReS measurements were prepared on top of silicon wafers through spin-coating and floating films off of glass onto a water surface. A top layer of d-PS-high was used as a support film to prevent the low molecular weight PS layers from breaking during the "floating off" process. As shown in Figure 3, d-PS-high and d-PS were separately spin-coated onto glass plates while h-PS was spin-coated onto a silicon wafer (step 1). These films were dried under vacuum at room temperature for about 1 day. The d-PS-high layer (typically 70 nm thick) was floated off on the surface of DI water (step 2). Then the floated film was picked up from above by the d-PS-coated glass substrate (step 3). This bilayer of d-PS-high/d-PS was floated off again on a water surface (step 4). In this step, the d-PS-high film works as a mechanical support for the weak d-PS film. Finally, this floating film was picked up by h-PS-coated silicon wafer from the bottom (step 5). The obtained trilayers were dried under vacuum at room temperature for at least 3 days.

Sample annealing for the FReS measurements was done in a specially designed oven which has small slots just large enough to fit silicon wafers of 1 in. diameter. This allowed the rapid temperature jumps (temperature equilibrium established in about 30 s) needed for short annealing times. Annealing temperatures are accurate to better than 1 °C.

Forward Recoil Spectrometry. FReS measurements were performed at the Ion Beam Analysis Facility at the University of Minnesota. FReS measures the concentration profiles of hydrogen and deuterium in the sample. A 3.0 MeV He^{2+} ion beam was incident on each sample at an angle of 15°, and an energy-sensitive detector with a 12 μm Mylar stopping foil was placed at an angle of 30° to the beam direction. This geometry allowed a depth of ~700 nm to be profiled with a depth resolution of about 80 nm. The beam current was set between 10 and 15 nA, and 10 μC of charge was collected for each spectrum, over 10−15 min. The FReS spectra were converted from yield vs energy to volume fraction vs depth using standard FReS analysis procedures.[24,25] In fitting the FReS data, we set the ratio of the recoil cross sections for H and D to be 1.44. This value was determined from the FReS data for a single layer of d-PS, taking the ratio of deuterium to hydrogen in the sample as 10.1, in accord with the MALDI−TOF results. In modeling the FReS data, we made use of a Gaussian convolution function with a correction for energy straggling inside the sample. The standard deviation of the Gaussian (σ) was taken to be a function of the depth x of the recoiled particles (H or D):

$$\sigma^2 = \sigma_0^2 + \frac{(a\Omega_B)^2}{(dE/dx)^2} \quad (1)$$

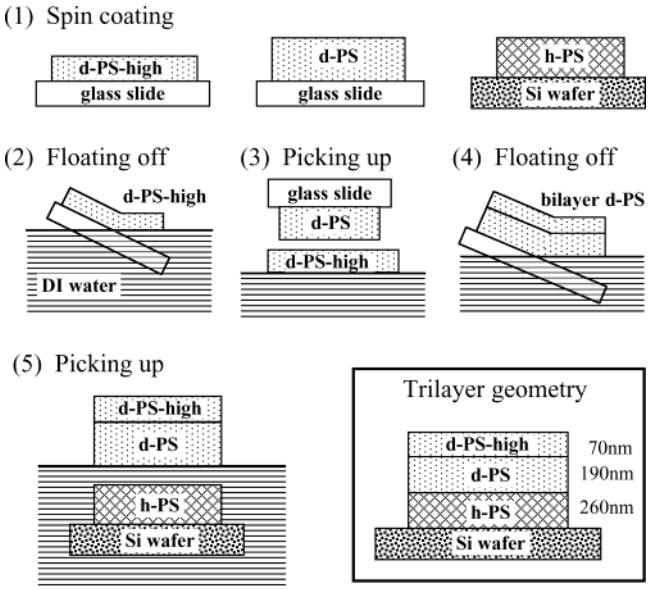

Figure 3. Schematic representation of trilayer film construction and typical sample geometry.

Here the first term σ_0 corresponds mainly to the broadening associated with the Mylar film (used to stop He nuclei) while the second term corrects for the gradual energy spread as particles lose energy inside the sample layer by the energy straggling (ES) effect. The Ω_B represents the Bohr energy straggling[26] which scales as the square root of x, E is the detected energy of H or D, and a is an adjustable parameter. For Ω_B, both contributions of the ingoing and the outgoing particles (He and H or D) were included according to ref 27. Here we took σ_0 to be 40 nm and a to be 4.38 for all fitting. Fitting without the energy straggling term altered the determined diffusion coefficients by at most 15%.

There are potential artifacts whose effects could mimic those of the energy straggling correction (eq 1). For example, if the low molecular weight polystyrene films developed very fine cracks, it might be possible for a small amount of interfacial broadening to occur even for an unannealed sample. We cannot discount this possibility, but given the negligible impact of the energy straggling term on the resulting diffusion coefficients, we have not undertaken to resolve the issue. Typical diffusion distances in the FReS measurements are 50−100 nm.

NMR. Nonspectroscopic pulsed-gradient spin-echo proton NMR was used to measure the self-diffusion coefficient of pure h-PS at high temperature (from 156 to 308 °C). A description of the measurement methods and data analysis practices appears in ref 28. The echo attenuations were successfully described in terms of a diffusivity distribution in accordance with the sample's known polydispersity ratio. Typical diffusion distances in the NMR measurements are 0.2−2 μm.

Rheometry. The rheological properties of h-PS were measured in oscillatory shear flow with a stress rheometer (SR-200, Rheometric Scientific, Inc.) using parallel plates of 8 and/or 25 mm diameter from 62 to 216 °C. The data are represented as the frequency-dependent complex viscosity η^* ($=\eta' + i\eta''$). At low temperatures, some error is introduced by the torsional compliance of the instrument. Here we use only the zero shear viscosities η' ($\omega \rightarrow 0$) which are not significantly affected by this error.

Results

Diffusion Coefficients. Figure 4 shows typical concentration profiles $C_D(x)$ and $C_H(x)$ obtained by FReS measurement for an unannealed trilayer film, along with the fitted curves (solid lines). The parameters used in this fit are the thicknesses of the three layers (70 nm for d-PS-high, 190 nm for d-PS, and 260 nm for h-PS) and the ratio of deuterium to hydrogen in each

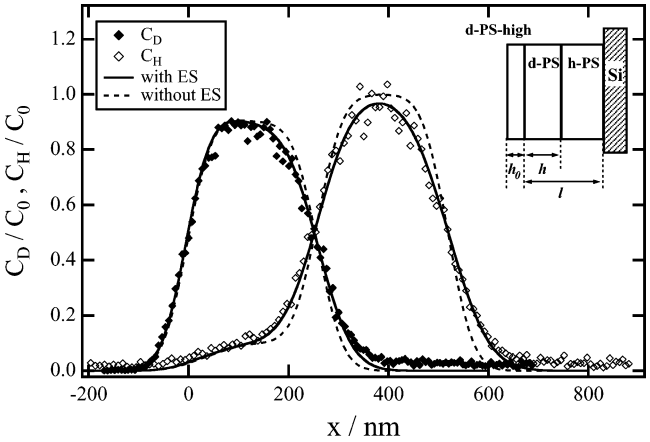

Figure 4. Concentration profiles of an *unannealed* trilayer sample whose geometry is depicted in the inset. C_D and C_H are the atomic densities of D and H in the sample film, respectively. C_0 is the atomic density of D in pure d-PS (C_8D_8) and the atomic density of H in pure h-PS (C_8H_8), both of which are equal to 4.81×10^{22} atoms cm^{-3}. The thicknesses of the layers, as determined by fitting, were $h_0 = 70$ nm (d-PS-high), $h = 190$ nm (d-PS), and $l - h = 260$ nm (h-PS).

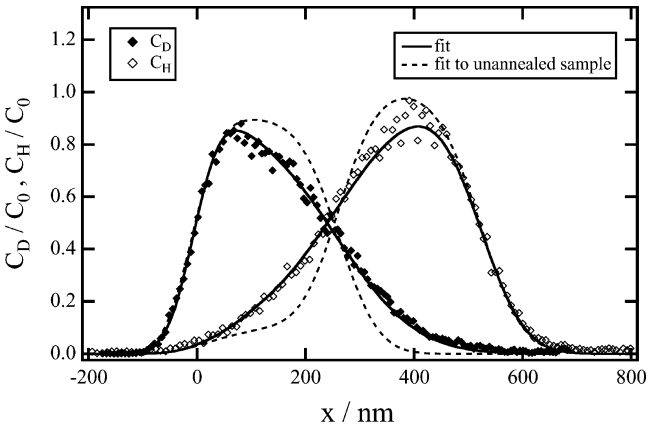

Figure 5. Concentration profiles of a trilayer film annealed at 84.3 °C for 420 s. Solid lines represent the fit to the diffusion equation with $D = 1.2 \times 10^{-13}$ cm^2 s^{-1}. The parameters h_0, h, and l are the same shown in Figure 4. The dashed lines represent the fit to the unannealed sample.

layer. For unannealed samples, the best fit thicknesses were always within 10% of the values determined by ellipsometry on single layer films (before assembling the trilayer). The ratio of deuterium to hydrogen for the two deuterated polymers was determined by MALDI−TOF (for d-PS) and by FReS on a single layer (for d-PS-high). The solid and dashed lines in the figure correspond to fitting with and without the energy straggling (ES) correction shown in eq 1. The fit with the ES correction is excellent. The details of the fitting procedure are given in the Appendix.

Figure 5 shows typical FReS results for an annealed trilayer (data points and solid line) with the dashed line showing the corresponding fit for the unannealed sample. This sample was annealed for 420 s at 84.3 °C. In fitting data on annealed samples, we have allowed the interface between d-PS and h-PS to broaden as described by Fickian diffusion (see Appendix).[29] The single fitting parameter is the diffusion coefficient D, since the layer thicknesses are determined from fits to the unannealed trilayer. Furthermore, the correlations between D and layer thickness values were found to be very weak, and thus any error in the thicknesses hardly influences the

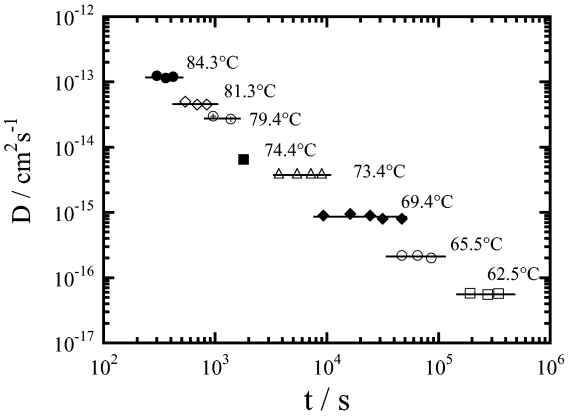

Figure 6. Diffusion coefficients for h-PS as a function of annealing times for various temperatures. The independence of D on annealing time is expected for Fickian diffusion in this thermodynamically ideal mixture.

resulting D values. The interface between d-PS-high and d-PS does not broaden for the annealing conditions used; this was verified by annealing a bilayer of h-PS and d-PS-high for 600 s at 84.3 °C. This result is reasonable given the higher T_g of d-PS-high sample. Reflecting boundary conditions[29] were utilized at the h-PS/Si and d-PS/d-PS-high interfaces; annealing times were sufficiently short that the influence of the boundary conditions on the fitted curves was small. The reported D values are reproducible to within 20%; we estimate the absolute accuracy to be better than 50%.

The annealing time dependences of the diffusion coefficients determined in this manner are shown in Figure 6. As can be seen in this figure, there is no time dependence, consistent with the assumption of Fickian diffusion. This is also consistent with the view that the measured D values are independent of the concentration, indicating that our d-PS and h-PS samples are reasonably regarded as *thermodynamically* identical. According to Green and Doyle,[30] critical slowing down appears for d-PS/h-PS mutual diffusion in bilayer films when the molecular weight is very high. Consistent with our results, they report that this effect is small for $M_w < 10^6$ g/mol. The very similar molecular weights and T_g values shown in Table 1 indicate the d-PS and h-PS samples are also *dynamically* very similar. Thus, the interdiffusion coefficients measured in the FReS experiment should be very similar to the self-diffusion coefficient for h-PS. We will not distinguish between these quantities for the remainder of this report.

Viscosity Measurements. Figure 7 shows the frequency dependence of the viscosity η' ($=G''/\omega$) measured at various temperatures. From these data zero shear viscosities were determined as $\eta'(\omega \rightarrow 0)$, as depicted by horizontal lines in the figure.

Discussion

Comparison of the Temperature Dependence of D and η. The Stokes−Einstein relation predicts that the diffusion coefficient of a sphere in a viscous continuum should be proportional to T/η, where η is the solvent viscosity. While the conditions assumed in the derivation of the Stokes−Einstein relation are not satisfied for the self-diffusion of a polymer chain, it is nevertheless instructive to compare the temperature dependences of these two quantities as both D and η are measures of the slowing down which occurs when the temperature of a polymer melt is lowered toward

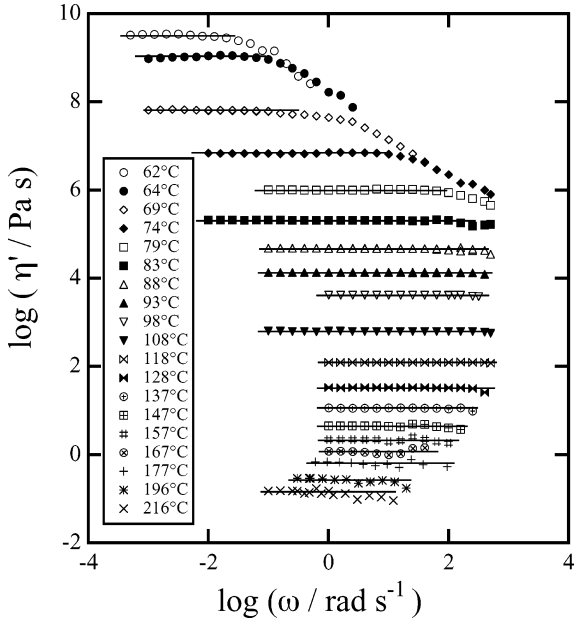

Figure 7. Shear viscosity η' for h-PS as a function of angular frequency ω at several temperatures.

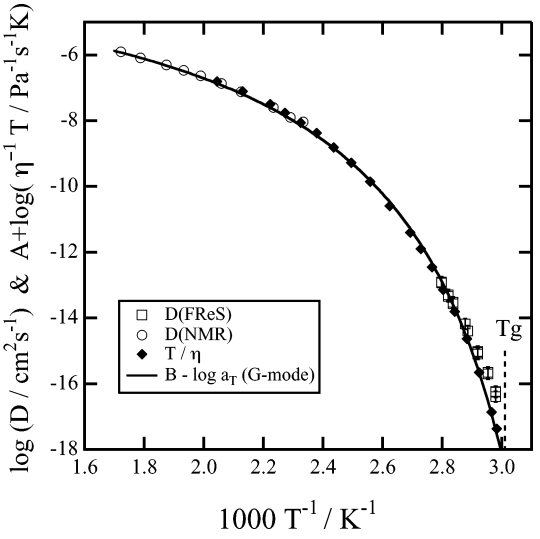

Figure 8. Comparison of D and T/η for h-PS as a function of inverse temperature. FReS measurements (made on d-PS/h-PS) and NMR measurements (on pure h-PS) are displayed. For comparison, T/η for pure h-PS is superposed on the D data in the form of $A + \log(T/\eta)$ with $A = -10.35$. The solid line represents the WLF equation reported by Inoue et al.[32,33] which was shifted vertically to overlap with T/η in the form of $B - \log a_T$ ($B = -14.28$).

T_g. Molecular theories of polymer melt dynamics, such as the Rouse model, also predict that D and η have essentially the same temperature dependence.

The logarithms of the diffusion coefficients determined by FReS (low temperature) and NMR (high temperature) are plotted against inverse temperature in Figure 8. For comparison, the temperature divided by the experimentally determined zero shear viscosity is also plotted, with an arbitrary vertical shift. The diffusion coefficients determined by FReS and NMR are smoothly connected, and this function almost follows the temperature dependence of T/η. However, below T_g + 25 °C, there is measurable decoupling between these two quantities, amounting to a total discrepancy of 1 decade out of the 10 decades spanned by the diffusion measurements.

Influence of Spatially Heterogeneous Dynamics on Diffusion? In low molecular weight glass formers, the breakdown of the Stokes−Einstein relation has been taken as an indication of spatially heterogeneous dynamics.[6,11] For example, the self-diffusion coefficients of TNB (1,3-bis(1-naphthyl)-5-(2-naphthyl)benzene)[8] have been reported over a wide temperature range down to T_g; D changes by 9 decades in a temperature range where T/η changes by almost 12 decades. Figure 8 shows that these two quantities are more similar for low molecular weight polystyrene but do retain distinct temperature dependences near T_g. Does this difference indicate the influence of spatially heterogeneous dynamics? We believe that the answer is "not necessarily". It has been known for more than 30 years that the segmental and terminal (global) dynamics of PS have different temperature dependences near T_g.[31] Because the PS chains studied here are short, η is dominated by segmental dynamics while D of course measures global dynamics. In the next three paragraphs we show that the different temperature dependences of D and η in Figure 8 can be quantitatively accounted for by the different temperature dependences of terminal and segmental dynamics.

Inoue et al. have separated the viscoelastic relaxation spectrum of unentangled polymers into global (Rouse or R-mode) and segmental contributions (glass or G-mode).[32] They have fit the two shift factors for the R- and G-modes with the WLF equation:

$$\log a_T = -\frac{c_1(T - T_r)}{c_2 + T - T_r} \qquad (2)$$

The parameters found for PS are $c_1 = 9.76$, $c_2 = 60.45$ (R-mode) and $c_1 = 10.37$, $c_2 = 56.11$ (G-mode) when the reference temperature, T_r, was chosen to be T_g + 12.2 °C.[32,33] One can expect that η/T should have the same temperature dependence as the G-mode for such short chains. Indeed, eq 2 provides an excellent representation of our viscosity data if T_r is chosen to be T_g + 16.5 °C, as shown by the solid line in Figure 8; the 4 K difference can be attributed to errors in determining T_g.

Since η/T for this low molecular weight polymer tracks the segmental relaxation times, we can see that the comparison of this quantity with the temperature dependence of D is not a test for the importance of spatially heterogeneous dynamics. What test would be appropriate? In low molecular weight glass formers such as *o*-terphenyl,[5,6] D and the rotational correlation time τ_c have different temperature dependences, such that the product $D\tau_c$ can increase by several orders of magnitude as T_g is approached from above. Qualitatively, this is understood to result from the different manner in which these observables are averaged. D is measured on long time and distance scales after a molecule has sampled many different dynamic environments. On the other hand, τ_c is measured on a shorter time scale such that molecules may not have changed dynamic environments. For polymers, the analogous quantities are D and τ_{term}: D represents center-of-mass translational motion, and τ_{term} is closely related to the reorientation of the end-to-end vector of the chain.[34] While both of these quantities reflect the global motion of the polymer chains, D is measured on longer time scales such that any influence of spatially heterogeneous dynamics would be averaged.

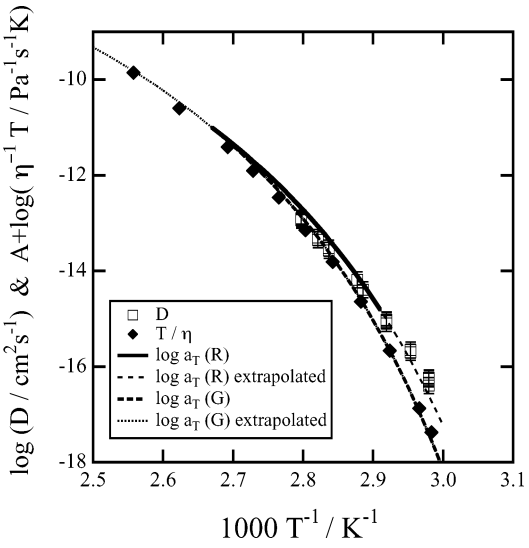

Figure 9. Comparison of diffusion coefficient with the Rouse mode shift factor (thick solid line) reported by Inoue et al.[32,33] The close agreement shows that the temperature dependence of the diffusion coefficient is consistent with the temperature dependence of the terminal relaxation time.

If spatially heterogeneous dynamics were strongly influencing diffusion in low molecular weight PS, we would expect D and τ_{term} to have different temperature dependences. Using the data of Inoue,[32,33] we can test this since the temperature dependence of their R mode should be the temperature dependence of τ_{term}. The results are shown in Figure 9; we have indicated the temperature range over which information about these modes is directly available from experiment. Within error, the R-mode (and τ_{term}) and D have the same temperature dependence at low temperature. At higher temperatures, it is known that the R- and G-modes have the same temperature dependence.[31] This is consistent with the behavior shown in Figure 8 above $T_g + 15$ K. Taken altogether, these comparisons indicate that for these low molecular weight polystyrene chains global rotational and translational motions have the same temperature dependences over a 10 decade range above T_g.

Why are D and τ_c uncoupled for low molecular weight glass formers like TNB and *o*-terphenyl, while the analogous quantities measuring rotational and translation motion in oligomeric polystyrene (D and τ_{term}) have the same temperature dependence? We attribute this difference to the molecular size. According to solid-state NMR measurements, the typical size of a slow region in polymeric and nonpolymeric glass formers near T_g is 1−4 nm.[19−22] The average end-to-end distance of the polystyrene chains used in this study is 3 nm. Assuming that the heterogeneity size in polystyrene is comparable to other glass-forming systems, we believe that an averaging effect associated with the large molecular size makes the enhancement of translational motion in polymeric systems very small. If this explanation is correct, then no enhancement of translational motion (relative to the terminal relaxation time) should be expected for high molecular weight polymer chains.

Does this mean that spatially heterogeneous dynamics has no influence on polymer self-diffusion? As we discussed above, terminal and segmental relaxation times in polymer melts are known to have distinct temperature dependences near T_g; i.e., time−temperature superposition is not obeyed in this temperature regime.[31] A number of suggestions have been made for the origin of this behavior,[35] including spatially heterogeneous dynamics.[36] The results presented here do not shed any light on the origin of the breakdown of time−temperature superposition. It is possible that heterogeneous dynamics indirectly influence polymer self-diffusion in this manner. Our point in this paper is that heterogeneous dynamics do not enhance translational diffusion relative to other observables sensitive to global chain dynamics.

Veniaminov et al. recently reported self-diffusion measurements of high molecular weight PMMA both above and below T_g.[9] They found significant translational displacements at very long times even at T_g − 20 °C and raised the possibility that this enhanced translational motion was due to spatially heterogeneous dynamics. While the use of different polymers precludes any direct comparison between our work and ref 9, our results would suggest that, at least for polystyrene, spatially heterogeneous dynamics is unlikely to be responsible for enhanced translational diffusion (relative to terminal relaxation) of high molecular weight chains at any experimentally accessible temperature.

As discussed in the Introduction, recent computer simulations by Varnik and Binder[10] show that the diffusion coefficient of a short polymer has a slightly weaker temperature dependence than does the viscosity. To compare our data to these simulations, we converted simulation temperature to real temperature using the T_c values which have been obtained by fits to the mode-coupling theory ($T_c \sim 400$ K for this molecular weight of PS). With this conversion, the temperature range where our D and η measurements overlap the simulation is 430−490 K. In our data, $D\eta/T$ increases by about 0.1 decade as the temperature decreases from 490 to 430 K. Unfortunately, when the experimental error bars are considered, this increase is consistent with either the change seen in the simulation or no change whatsoever over this small temperature range.

Concluding Remarks

A number of observations about dynamics near T_g in polymeric systems have been explained by the presence of spatially heterogeneous dynamics, including the nonexponential correlations functions associated with segmental relaxation and the unexpected large diffusion coefficients for low molecular weight probes in polymer matrices. Here we tested whether this heterogeneity might also enhance the center-of-mass diffusion of polymer chains. We found that the measured diffusion coefficients for polystyrene chains with degree of polymerization about 17 had nearly the same temperature dependence as T/η. The small discrepancy was attributed to the different temperature dependences for terminal and segmental relaxation in polystyrene. A more appropriate test for the influence of spatially heterogeneous dynamics compares diffusion with the terminal relaxation time. The two quantities exhibit the same temperature dependence over 10 orders of magnitude in diffusion coefficients, indicating that the center-of-mass diffusion of even short polystyrene chains is not enhanced due to heterogeneous dynamics.

In contrast to our findings for polymer self-diffusion, spatially heterogeneous dynamics are thought to have a strong influence on the diffusion of small probes in polymeric matrices and the self-diffusion of low molec-

ular weight glass formers (e.g., TNB and *o*-terphenyl). These differences are attributed to the size of the diffusing species. When the diffusing molecule is comparable to the size of the heterogeneities (a few nanometers), it effectively experiences an average environment, either because it simultaneously experiences multiple environments (but cannot take advantage of the fast regions) or because its size makes it move so slowly that even if it is entirely inside a fast region, it can make very little progress before the environment becomes slower. If this explanation is correct, the result that polymer self-diffusion is not enhanced relative to terminal relaxation should be generally applicable to polymers other than polystyrene.

Acknowledgment. We are grateful to K. Crowley and G. D. Zografi for the use of their DSC instrument and to M. M. Vestling for performing the MALDI−TOF measurements. We thank Y. Wang (University of Minnesota) for his help with FReS measurements, Thomas Mourey for SEC molecular weight characterization, and Kurt Binder, Russ Composto, and Paul Nealey for helpful discussions. This work was supported by the National Science Foundation (CHE-0245674). O.U. acknowledges the financial support from the Ministry of Education, Culture, Sports, Science and Technology, Japan, for supporting his stay in the US.

Appendix

The concentration profiles $C_D(x)/C_0$ and $C_H(x)/C_0$ for unannealed trilayers are written as

$$C_D(x)/C_0 = \phi_{d-PS-high}\Psi(0,h_0) + \phi_{d-PS}\Psi(h_0, h_0 + h),$$

$$C_H(x)/C_0 = (1 - C_D(x)/C_0)\Psi(0, h_0 + l) \quad \text{(A-1)}$$

where l, h, and h_0 are thicknesses depicted in the inset of Figure 4, and ϕ_{d-PS} and $\phi_{d-PS-high}$ are the mole fractions of D (relative to the total amount of D and H) in d-PS and d-PS-high, respectively. The D content in d-PS was determined as $\phi_{d-PS} = 0.91$ from the MALDI−TOF result. On the other hand, $\phi_{d-PS-high}$ was determined as 0.95 from the FReS measurement for a single-layered d-PS-high film on Si wafer. $\Psi(0,h)$ in eq A-1 represents a rectangular function defined as $\Psi = 1$ for $x = 0 \sim h$ and 0 for $x < 0$, $x > h$. Through the use of the following convolution equation the curves in Figure 4 were calculated.

$$F(x) = \int_{-\infty}^{\infty} C(x)G(\mu - x)\, d\mu \quad \text{(A-2)}$$

Here x is the depth measured from the surface inside the sample, $C(x)$ corresponds to either C_D and C_H, and $G(x)$ is the Gaussian distribution function that represents the instrumental resolution:

$$G(\mu - x) = \frac{1}{\sqrt{4\pi\sigma}} \exp\left\{-\frac{(\mu - x)^2}{2\sigma^2}\right\} \quad \text{(A-3)}$$

where σ corresponds to the depth resolution of FReS represented by eq 1.

To analyze the concentration profile of the annealed trilayer, Fickian solutions to the diffusion equation in a finite system were used:

$$C_D(x,t)/C_0 = \phi_{d-PS-high}\Psi(0,h_0) + \frac{\phi_{d-PS}\Psi(h_0,h_0 + l)}{2}\sum_{n=-\infty}^{\infty}\left[\mathrm{erf}\left(\frac{h + 2nl - (x - h_0)}{\sqrt{4Dt}}\right) + \mathrm{erf}\left(\frac{h - 2nl + (x - h_0)}{\sqrt{4Dt}}\right)\right],$$

$$C_H(x,t)/C_0 = (1 - C_D(x,t)/C_0)\Psi(0,h_0 + l) \quad \text{(A-4)}$$

where the second term in $C_D(x,t)$ corresponds to the Fickian solution and D is the interdiffusion coefficient. These equations and eq A-2 were used to calculate the solid curves shown in Figure 5.

References and Notes

(1) Ediger, M. D. *Annu. Rev. Phys. Chem.* **2000**, *51*, 99.
(2) Sillescu, H. *J. Non-Cryst. Solids* **1999**, *243*, 81.
(3) Schmidt-Rohr, K.; Spiess, H. *Phys. Rev. Lett.* **1991**, *66*, 3020.
(4) Tarjus, G.; Kivelson, D. *J. Chem. Phys.* **1995**, *103*, 3071.
(5) Cicerone, M. T.; Ediger, M. D. *J. Chem. Phys.* **1996**, *104*, 7210.
(6) Cicerone, M. T.; Wagner, P. A.; Ediger, M. D. *J. Phys. Chem. B* **1997**, *101*, 8727.
(7) Hall, D. B.; Dhinojwala, A.; Torkelson, J. M. *Phys. Rev. Lett.* **1997**, *73*, 109.
(8) Swallen, S. F.; Bonvallet, P. A.; McMahon, R. J.; Ediger, M. D. *Phys. Rev. Lett.* **2003**, *90*, 015901.
(9) Veniaminov, A. V.; Sillescu, H. *Macromolecules* **1999**, *32*, 1828.
(10) Varnik, F.; Binder, K. *J. Chem. Phys.* **2002**, *117*, 6336.
(11) Heuberger, G.; Sillescu, H. *J. Phys. Chem.* **1996**, *100*, 15255.
(12) Tao, H.; Lodge, T. P.; von Meerwall, E. D. *Macromolecules* **2000**, *33*, 1747.
(13) Green, P. F. Ion Beam Analysis of Diffusion in Polymer Melts. Ph.D. Thesis, Cornell University, 1985; Chapter 3.
(14) Mills, P. J.; Green, P. F.; Palmstrom, C. J.; Mayer, J. W.; Kramer, E. J. *Appl. Phys. Lett.* **1984**, *45*, 9.
(15) Zhao, X.; Zhao, W.; Sokolov, J.; Rafailovich, M. H.; Schwarz, S. A.; Wilkens, B. J.; Jones, R. A. L.; Kramer, E. J. *Macromolecules* **1991**, *24*, 5991.
(16) Russell, T. P.; Karim, A.; Mansour, A.; Felcher, G. P. *Macromolecules* **1988**, *6*, 1890.
(17) Karim, A.; Felcher, G. P.; Russell, T. P. *Macromolecules* **1994**, *27*, 6973.
(18) Brandup, J.; Immergut, E. H. *Polymer Handbook*, 3rd ed.; Wiley-Interscience: New York, 1989; Chapter VII.
(19) Tracht, U.; Wilhelm, M.; Heuer, A.; Feng, H.; Schmidt-Rohr, K.; Spiess, H. W. *Phys. Rev. Lett.* **1998**, *81*, 2727.
(20) Tracht, U.; Wilhelm, M.; Heuer, A.; Spiess, H. W. *J. Magn. Reson.* **1999**, *140*, 460.
(21) Reinsberg, S. A.; Qiu, X. H.; Wilhelm, M.; Spiess, H. W.; Ediger, M. D. *J. Chem. Phys.* **2001**, *114*, 7299.
(22) Qiu, X. H.; Ediger, M. D. *J. Phys. Chem. B* **2003**, *107*, 459.
(23) Santangelo, P. G.; Roland, C. M. *Macromolecules* **1998**, *31*, 4581.
(24) Doyle, B. L.; Brice, D. K. *Nucl. Instrum. Methods* **1998**, *B35*, 301.
(25) Composto, R. J.; Walters, R. M.; Genzer, *J. Mater. Sci. Eng.* **2002**, *R38*, 107.
(26) Bohr, N. *Mater. Fys. Medd. Dan. Vid. Selsk.* **1948**, *18* (8).
(27) Turos, A.; Meyer, O. *Nucl. Instrum. Methods* **1984**, *B4*, 92.
(28) Shim, S. E.; Parr, J.; von Meerwall, E.; Isayev, A. I. *J. Phys. Chem. B* **2002**, *106*, 12072.
(29) Crank, J. *The Mathematics of Diffusion*; 2nd ed.; Oxford University Press: Oxford, 1975; p 16.
(30) Green, P. F.; Doyle, B. L. *Macromolecules* **1987**, *20*, 2471.
(31) Plazek, D. J. *J. Phys. Chem.* **1965**, *69*, 3480.
(32) Inoue, T.; Onogi, T.; Osaki, K. *J. Polym. Sci., Part B: Polym. Phys.* **1999**, *37*, 389.
(33) Inoue, T. Private communication, 2002.
(34) Adachi, K.; Yoshida, H.; Fukui, F.; Kotaka, T. *Macromolecules* **1990**, *23*, 3138.
(35) Ngai, K. L.; Plazek, D. J.; Rendell, R. W. *Rheol. Acta* **1997**, *36*, 307.
(36) Ilan, B.; Loring, R. F. *J. Chem. Phys.* **2000**, *112*, 10588.

MA0352025